Development of the L-type CaV / BK Complex Simulator (I): electrophysiological interaction

Marleni Reyes Monreal
PhD student in History
(Instituto de Ciencias Sociales y Humanidades BUAP)
PI. School of Visual and Audiovisual Arts (ARPA), BUAP.
Complejo Cultural Universitario (CCU). Puebla, Pue. México.
E-mail: marleni.reyes@correo.buap.mx

Jessica Quintero Pérez
PhD student in Biomechanics and Bioengineering Applied to Health (Universidad de Alcalá, España).
PHC. Degree in Physiotherapy-Faculty of Medicine.
Benemérita Universidad Autónoma de Puebla (BUAP).
Health area. Puebla, Pue. México.
E-mail: jessica.quintero@correo.buap.mx

Miguel Felipe Pérez Escalera
PhD student in Computer Sciences
(Universidad de las Américas UDLAP)
PI. School of Visual and Audiovisual Arts (ARPA), BUAP.
Complejo Cultural Universitario (CCU). Puebla, Pue. México.
E-mail: miguel.escalera@correo.buap.mx

Arturo Reyes Lazalde
PhD in Basic Biomedical Research (UNAM)
PI. Holder of the Faculty of Biological Sciences, BUAP.
Ciudad Universitaria. Puebla, Pue. México.
E-mail: arturoreyeslazalde@yahoo.com.mx

María Eugenia Pérez Bonilla
PhD in Experimental Pathology (CINVESTAV-IPN, Mx) PI. Holder of the Faculty of Biological
Sciences, BUAP.
Ciudad Universitaria. Puebla, Pue. México.
E-mail: maria.perez@correo.buap.mx

ABSTRACT
Complexes formed by voltage-activated calcium channels (CaV) and high-conductance potassium channels activated by Ca^{2+} (BK) have been studied in smooth muscle, secretory cells and in synaptic terminals, where they regulate muscle contraction, secretory activity, and neurotransmission. However, the complex formed by L- type CaV channels and BK in the soma has been poorly treated. Based on immunostaining studies showing the coexistence of these channels in the neuron soma, their possible interaction was theoretically studied. Two simulators based on the Hodgkin and Huxley formalism were developed to perform virtual experiments on current and voltage clamp. The mathematical models were implemented in Visual Basic® 6.0 and were solved numerically. The results indicate that the BK channels

were activated with internal Ca^{2+} at μM concentrations. The BK channels follow the kinetics of L-type CaVs. The interaction of L-type CaV – BK complex in the soma produced a decrease in neuronal excitability.

Keywords: Simulators, BK channels, L-type CaV channels, Neuronal excitability

1 INTRODUCTION

1.1 BK CHANNELS

Calcium and voltage-gated high-conductance K channels (BK channels) are ubiquitously expressed in a wide variety of neurons (Contet et al., 2016) and non-tissue neurons where they play an important role in the regulation of physiological processes such as the modulation of smooth muscle contraction, secretion, cardiac pacemaker frequency, neurotransmitter release, control of neuronal firing patterns and neuronal excitability, (Ha & Cheong, 2017; Jackson, 2018; Kshatri et al., 2018). At a cellular level, they are located in synaptic terminals, dendrites, axon, and soma (Misonou et al., 2006). In the soma, the pyramidal neurons show two distinct types of localization, a scattered and a groups pattern (Kaufmann et al., 2009). The clinical relevance of dependence on these channels has been reported in several diseases such as benign familiar neonatal seizure, episodic ataxia, epilepsy, and chronic pain (Contet et al., 2016). The role of BK channels in epilepsy is controversial and is a growing area of intense research. These channels are associated with voltage-gated calcium channels (CaV) distributed in somatodendritic gradients. They are associated with P/Q type CaV in different somatic coclustering in Purkinje neurons (Indriati et al., 2013). The association in the soma of L-type CaV with BK channels has been little studied.

BK is encoded by a single gene (*KCNMA1, SLO-1*), it is made up of four alpha subunits and has 7 transmembrane subunits (Lee & Cui, 2010). Two different classes of auxiliary subunits have been identified: β subunit and γ subunit. It has been intensively investigated and established that β (β1-β4) subunits modulate the activity of the BK channel (Li & Yan, 2016). These channels have a high conductance per single channel ~250 pS (100-300 pS) (at symmetric K^+ concentrations) (Butler et al., 1993). They open in response to the depolarization of the membrane, due to an increase in the internal calcium concentration ($[Ca^{2+}]_i$) or because of both (Ramon Latorre et al., 2017). The BK channel has been reported to have two putative calcium-binding sites located in the RCK2 and RCK1 domains (Lee & Cui, 2010). Subunits modulate BK channels (Contet et al., 2016). The activation voltage for the BK channel depends on $[Ca^{2+}]_i$ (Miranda et al., 2018). Brenner et al (2000) found that at a membrane potential ~100 mV, BK channels become activated with $[Ca^{2+}]_i$ at concentrations ≥ 10 μM. The affinity of BK channels for Ca^{2+} ranges from 1 to 10 μM (Contreras et al., 2013). These channels contribute to the repolarization of the action potential (AP) and mediate the rapid phase of post-hyperpolarization (fAHP) that follows the

AP (Lancaster & Nicoll, 1987). The K^+ output current tends to hyperpolarize the cell and attenuates the effect of the excitatory stimuli.

1.2 L-TYPE VOLTAGE-GATED CALCIUM CHANNELS

Ca^{2+} is an ion of utmost importance for cells. In general, it is a signaling system. It converts electrical signals into chemical signals and its response depends on the specific cell type: secretion, metabolism, cell proliferation, contraction, excitability, and gene expression. (Bean, 1989). $[Ca^{2+}]_i$ comes from two sources: influx by voltage-gated Ca^{2+} channels (CaV) and by the efflux of the reticular system (endoplasmic or sarcoplasmic). In neurons, there are various types of voltage-gated Ca^{2+} channels. Due to their biophysical and pharmacological characteristics, they can be classified into 5 families: T-type, L-type, N-type, P/Q-type, and R-type Ca^{2+} (Tsien et al., 1988). Specifically, the L-type channels have a ~25 pS conductance, do not significantly activate during the depolarization of hundreds of milliseconds, are sensitive to dihydropyridine, and have a very slow inactivation rate (τ >500 ms) (Tsien et al., 1988). L-type channels are located in a variety of neurons (Tsien et al., 1991) and are mainly located in the cell body and proximal dendrites (Hell et al., 1993). They have been studied mainly in secretory cells, cardiac muscle, and in neurons in the control of neurotransmission. In synaptic transmission, the distance between CaV and the receptor that initiates exocytosis can be ~50 nm (Augustine et al., 2003). They regulate synaptic plasticity and blockers such as nifedipine (dihydropyridine) would modulate brain function (Striessnig et al., 2006).

Electrophysiologically, there is interaction between the L-type voltage-gated calcium channel and the BK channel in a variety of neurons forming nanodomains (Vivas et al., 2017). In the suprachiasmatic nucleus, a differential contribution of calcium sources between day and night for the activation of BK current in the circadian clock has been demonstrated. L-type calcium channels are the primary source of calcium during the day for the activation of BK channels (Whitt et al., 2018). The coexistence and the activation of BK channels by L-type calcium channels have been studied in different tissues (Bellono et al., 2017; Vivas et al., 2017). The precise functional interaction between the CaV and BK channels remains unclear (Müller et al., 2007). The role of L-type calcium channel complexes and BK channels in the neuron soma has been sparsely addressed.

1.3 OBJECTIVE

The objective of this work are: (1) Develop simulators of the L-type CaV / BK complex, and (2) theoretically explore the interaction of the L-type CaV/BK complex in neuron soma, using simulators that allow virtual experiments under current and voltage clamp conditions.

2 MATERIAL AND METHODS

Two simulators were designed and developed for the theoretical study of the L-type CaV/BK channel complex in the somatic membrane. (1) Simulator for experiments with current clamp technique, (2) Simulator for experiments with the voltage clamp technique. The electrical activity of the neuron was reproduced with Hodgkin and Huxley formalism (Hodgkin & Huxley, 1952).

2.1 SIMULATORS OF THE L-TYPE CAV/BK COMPLEX FOR EXPERIMENTS IN VOLTAGE AND CURRENT CLAMP.

In the first simulator (voltage clamp) the somatic membrane has voltage dependent Na^+ and K^+ channels to generate a train of action potentials, described as a control condition and L-type CaV channels and BK channels are added to generate the experimental conditions that modify the AP train. In the second simulator (current clamp) the somatic membrane has L-type CaV channels and BK channels. The equations that integrate the model are the following (Hodgkin & Huxley, 1952; Sterratt et al., 2011) (Eqs. 1 to 10).

$$-C_m \frac{dV}{dt} = g_{Na}m^3h(V - E_{Na}) + g_K n^4(V - E_k) + g_L(V - E_L) + g_{Ca}m_{Ca}^2 h_{Ca}(V - E_{Ca}) + g_{BK} q (V - E_{BK}) \tag{1}$$

$$\frac{dm}{dt} = \alpha_m(V)(1 - m) - \beta_m(V) m \tag{2}$$

$$\frac{dh}{dt} = \alpha_h(V)(1 - h) - \beta_h(V) h \tag{3}$$

$$\frac{dn}{dt} = \alpha_n(V)(1 - n) - \beta_n(V) n \tag{4}$$

Where:

V is the voltage of the membrane and C_m is membrane capacitance. The conductances for sodium, potassium, leakage, L-type calcium and high-conductance calcium-dependent potassium are: g_{Na}, g_K, g_L, g_{Ca}, g_{BK} and E_{Na}, E_K, E_L, E_{Ca} E_{BK} are the corresponding to equilibrium potentials, m is the activation constant for Na^+, h is the inactivation constant for Na^+, n is the activation constant for K^+, m_{Ca} is the

activation constant for L-type Ca^{2+}, h_{Ca} is the inactivation constant for L-type Ca^{2+}, q is the activation constant for BK. The parameters used are: $E_{Na} = 115$, $E_K = -77$, $E_L = -54.4$ $E_{Ca} = 140$, $E_{BK} = -140$ (mV), $g_{Na} = 120$, $g_K = 36$ (mS/cm^2), $g_{Ca,}$ and g_{BK} (μS/cm^2) are designated by the simulator user.

The empirical equations for Na^+ and K^+ currents: α_m, β_m, α_n, β_n, α_h, and β_h are as follows (Eqs. 5 to 10).

$$\alpha_m = \frac{0.1\,(V+35)}{1-exp^{(-\frac{V+50}{10})}} \tag{5}$$

$$\beta_m = 4\,exp(-\frac{V+60}{18}) \tag{6}$$

$$\alpha_h = 0.07\,exp(-\frac{V+60}{20}) \tag{7}$$

$$\beta_h = 1/(1+exp(-\frac{V+30}{10}) \tag{8}$$

$$\alpha_n = \frac{0.01\,(V+50)}{1-exp\,(-\frac{V+50}{10})} \tag{9}$$

$$\beta_n = 0.125\,exp\left(\frac{V+60}{30}\right) \tag{10}$$

Where the velocity coefficients for Na^+ are α_m, β_m, α_h, β_h, and for K^+ are α_n and β_n.

Equations for the L-type Ca^{2+} current are the following (Pospischil et al., 2008) (Eqs. 11 to 15).

$$I_{Ca} = \bar{g}_{Ca}\,m_{Ca}^2\,h_{Ca}\,(V - E_{Ca}) \tag{11}$$

$$h_{Ca} = \frac{K}{K+[Ca^{2+}]_i}\ ,\ K=7.2 \tag{12}$$

$$\frac{dm_{Ca}}{dt} = \alpha_{m_{Ca}}\,(V)(1-m_{Ca}) - \beta_m m_{Ca} \tag{13}$$

The α_{mCa} and β_{mCa} are expressed empirically (Eqs 14 and 15).

$$\alpha_{m_{Ca}} = \frac{0.055(-27-V)}{exp\,(\frac{-27-V}{3.8}-1)} \tag{14}$$

$$\beta_{m_{Ca}} = 0.94 \exp\left(\frac{-75-V}{17}\right) \tag{15}$$

2.2 EQUATION TO CALCULATE $[Ca^{2+}]_i$ FROM THE Ca^{2+} CURRENT

Based on the work of Wang (1998), Eq. 16 was used to derive $[Ca^{2+}]_i$ from the Ca^{2+} current (Traub, 1982, 1991; Wang, 1998).

$$\frac{d[Ca^{2+}]_i}{dt} = \alpha_{Ca}\ I_{Ca} - \frac{[Ca^{2+}]_i}{\tau_{Ca}} \tag{16}$$

τ_{Ca} is the time constant of the buffering process and α_{Ca} is a constant. Helmchen et al. (1996) and Markram et al. (1995) propose a value for α of 0.002 (μM (ms μA)$^{-1}$ cm^2), with an influx of Ca^{2+} of ~200 nM per spike and a time constant τ_{Ca} of 80 ms.

2.3 EQUATIONS FOR BK CURRENT

The equations for the calculation of the BK current are (Eqs. 17 and 18):

$$I_{BK} = \bar{g}_{BK}\ q\ (V - E_{BK}) \tag{17}$$

$$\frac{dq}{dt} = \alpha_q(V)(1 - q) - \beta_q\ q \tag{18}$$

The α_q and β_q are expressed empirically (Eqs. 19 and 20).

$$\alpha_q = \frac{\exp\left(\frac{V}{27}\right)0.005\left(200 - [Ca^{2+}]_i\right)}{\exp\left(\frac{200 - [Ca^{2+}]_i}{20}\right) - 1} \tag{19}$$

$$\beta_q = 0.0004\ to\ 0.0002 \tag{20}$$

The type-L CaV/BK complex simulator for current and voltage clamp consider the pharmacological action of the BK channel blockers: iberiotoxin (Galvez et al., 1990) and charybdotoxin (Cui et al., 2009) and the L-type Ca^{2+} current blocker with nifedipinae (Striessnig et al., 2006), here reflected as a decrease in conductances for BK and L-type CaV, respectively.

The equations of the simulators were implemented in Visual Basic 6.0 for Windows® 7 to 10 environment and interfaces, which allow interactive experiments to be carried out in multiple experimental conditions, were designed. To start the integration, a fourth-order Runge-Kutta method with a step time of dt = 0.01 was used. An algorithm written in basic to solve differential equations with this method is found in Zill (Zill, 1988).

The simulators generate ASCII files to be exported to graphing and analysis programs. All data analysis was performed with Origin 6.0 graphing and curve fitting software, and the Levenberg-Marquardt algorithm was used to perform nonlinear least-squares fits. BK and CaV conductance-voltage (G-V) relations were determined from the amplitude voltage steps to the test voltage. Each G-V relation was then fitted with a Boltzmann function (Cox, 2014) (Eq. 25).

$$\frac{G}{G_{max}} = \frac{1}{1+\exp\left[\left(V_{\frac{1}{2}}-V\right)\frac{zF}{RT}\right]} \tag{25}$$
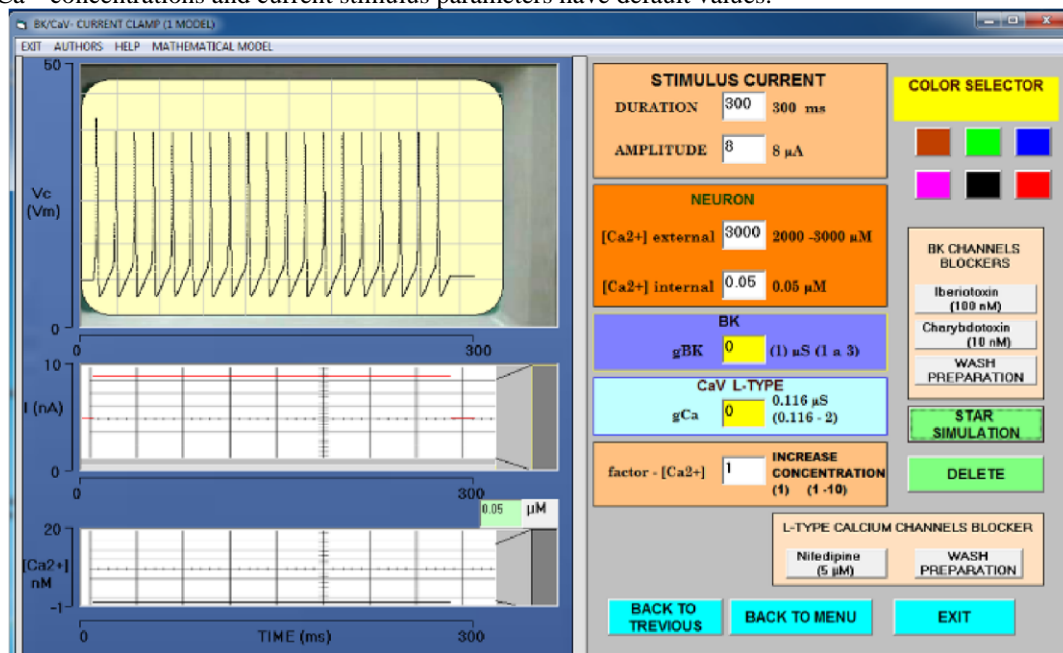
3 RESULTS

3.1 SIMULATOR INTERFACE AND CONTROL SIMULATION.

The simulator for the experiments with the current clamp technique is shown in Figure 1. It is divided into two sectors, one on the right side, for data entry: stimulus pulse, external and internal Ca^{2+} concentrations, conductances for the channels BK and L-type CaV, and a factor to inject Ca^{2+}. It has buttons for the application of blockers for the BK channel and the L-type CaV channel. Another on the left side, for the graphic recording of the simulations, where the oscilloscope screens are located for the display of the AP train (upper), the stimulus pulse (middle), and $[Ca^{2+}]_i$ reached by the opening of the type-L CaV channels (lower). The values of the parameters that appear in the interface when opening the simulator correspond to default values. The pulse of the current has a duration of 300 ms and an amplitude of 8 nA. $[Ca^{2+}]_e = 3$ mM, $[Ca^{2+}]_i = 0.05$ μM. The conductances for BK and L-type CaV are at zero. These conditions correspond to a control simulation: the neuron does not have BK or CaV channels. The AP train that is recorded corresponds to the electrical activity of a neuron with voltage-gated Na^+ and K^+ channels. BK channels have been reported to have their effect on a part of the posthiperpolarization of AP in the soma, but not on the apical dendrites in hippocampal pyramidal neurons. The authors indicate that this difference is determined by a non-uniform distribution of ion channels, suggesting a greater distribution of BK in the

soma (Poolos & Johnston, 1999). L-type CaV channels are located mainly in the cell body and proximal dendrites (Hell et al., 1993). In this simulator, the L-type CaV/BK complex is located in the soma.

Figure 1. CaV-L/BK simulator user interface. Electrophysiological simulation with the current clamp technique of a Hodgkin and Huxley type neuron in the absence of the type-L CaV /BK complex. The upper oscilloscope display shows the AP train under these conditions (control). The lower oscilloscope display shows the internal Ca^{2+} concentration (50 nM). The external and internal Ca^{2+} concentrations and current stimulus parameters have default values.
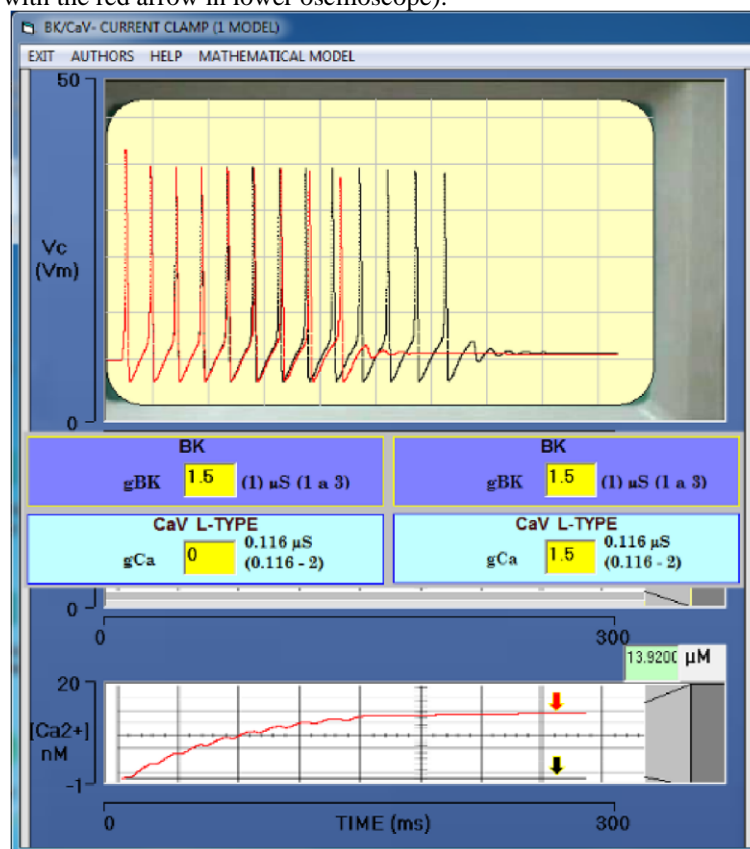

3.2 SIMULATION OF SENSITIVITY TO VOLTAGE AND INTERNAL CALCIUM CONCENTRATION.

BK channels are activated by voltage, by an increase in $[Ca^{2+}]_i$ or by both (Cui et al., 2009). Both stimuli converge allosterically in the activation of BK channels by increasing concentrations of $[Ca^{2+}]_i$ that shift the conductance and voltage curve (G-V) to the left (Cui et al., 1997). In this work, the contribution of the voltage in the opening of the BK channel was tested through the effect it has on the AP train. Figure 2, shows the electrophysiological simulation of a neuron stimulated with a pulse current with a duration of 300 ms and a current intensity of 8 nA. The external and internal Ca^{2+} concentrations are the same as those described in the control ($[Ca^{2+}]_e$ = 3 mM y $[Ca^{2+}]_i$ = 0.05 μM). The neuron has voltage-gated Na^+ and K^+ channels and BK channels in the cell membrane. CaV channels are absent (gCa = 0 μS). Under these experimental conditions, BK channels only respond to variations in membrane potential. The AP train ends in a shorter time (Figure 2, black trace) compared to the control (simulation in Figure 1). It can be seen how the frequency of AP decreases. Internal Ca^{2+} concentrations (≤100 nM) do not activate the channel. In the simulated case, $[Ca^{2+}]_i$ remains at 50 nM throughout the whole simulation time. This result agrees

with previous works, where it is shown that BK channels are primarily and independently commanded by voltage (Toro et al., 1998). BK channels are sensitive to the increase of internal calcium concentration in the micromolar order (Meera et al., 1996). In the soma, they regulate the firing in burst of PA. To explore the effect of the increase in internal Ca^{2+}, a simulation in a neuron with Na^+, K^+, BK, and L-type CaV channels was carried out. Under these conditions, the voltage-gated calcium channel opens with the depolarization of the membrane. An influx of Ca^{2+} occurs and internal Ca^{2+} increases in the order of micromolar. The simulation shows a slow increase of internal Ca^{2+} with respect to time until reaching a concentration of 13.9 µM (red curve, lower oscilloscope screen, Figure 2). This concentration of Ca^{2+} activates jointly with the voltage to the BK channels, an adaptation of the AP train occurs and a decrease in the neuronal excitability is observed (AP train, red line, Figure 2). These results are similar to those reported by Bock and Stuart (Bock & Stuart, 2016). The unique and singular properties of BK channels suggest that to be active, they must colocalize with Ca^{2+} channels and possess specialized sites for Ca^{2+} binding (Stefani et al., 1997). The analysis with a wide range of $[Ca^{2+}]_i$ reveals that the function of the BK channel is exquisitely modulated by Ca^{2+} (Meera et al., 1996).

Figure 2. Voltage and calcium sensitivity of BK channels. The upper oscilloscope screen shows the AP train simulations: a neuron with only voltage-activated BK (black trace) and a neuron with voltage-activated BK and internal Ca^{2+} (red trace). It is observed that the AP train ends in less time when the BK channel is activated with voltage and Ca^{2+} (it increases slowly until it reaches 13.9 µM, red trace with the red arrow in lower oscilloscope).

3.3 ACTION POTENTIAL ADAPTATION BY BK SIMULATION.

Figure 3, shows two simulations to compare the AP train of a control neuron (black line) against an experimental neuron with the type-L CaV/BK complex, with the following values for the variables: 0.116 (µS) for g_{Ca} and 1 (µS) for g_{BK} and a calcium concentration of 1.2 µM was reached (red trace). A decrease in firing frequency is observed. The frequency-time relationship of these two neurons and one more neuron with a type-L CaV/BK complex was determined, increasing g_{Ca} (gCa = 0.5 µS), gBK=1 µS (an internal calcium concentration of 4.87 µM was reached) (Figure 4). A decrease is clearly observed in the firing frequency of the neurons that have CaV type-L/BK compared to the control neuron. The adaptation percentage for the control neuron F_{adap} = 0 %, for the neuron with g_{Ca} = 0.0116 µS, F_{adap} = 12.7%; for the neuron with g_{Ca} = 0.5 µS, F_{adap} = 19%. (F_{adap} = (f$_0$-f$_{ss}$)/f$_0$, where f$_0$ is the initial frequency and f$_{ss}$ is the frequency in the steady state). A greater adaptation occurs with a greater $[Ca^{2+}]_i$ generated by a greater conductance of the type-L CaV channel. An adaptation process was studied in a theoretical model for cortical pyramidal cells (Wang, 1998). In this model, the adaptation percentage was much higher F_{adap} = 57%. In this case, the model is integrated by two compartments with an electrotonic junction and g_{Na} = 145 mS/cm^2. In our case, g_{Na} = 120 mS/cm^2. At a higher Na$^+$ conductance, the AP train presents a greater frequency and the adaptation percentage is greater. Theoretical and experimental results (Marcantoni et al., 2010) indicate that the action of the BK channel is to reduce the AP frequency and to decrease the excitability. The Ca^{2+} requirements of order µM for the BK channel to regulate the excitability, suggest a colocalization of the CaV – BK channels (Toro et al., 1998).

Figure 3. Simulation of AP train in neuron with BK and CaV-L. The black line corresponds to an AP train from a control neuron. The trace in red corresponds to the AP train in a neuron with $g_{BK} = 1$ µS, $g_{Ca} = 0.116$ µS, $[Ca2+]_i = 1.2$ µM, it is observed how the APs decrease their frequency and produce an adaptation.
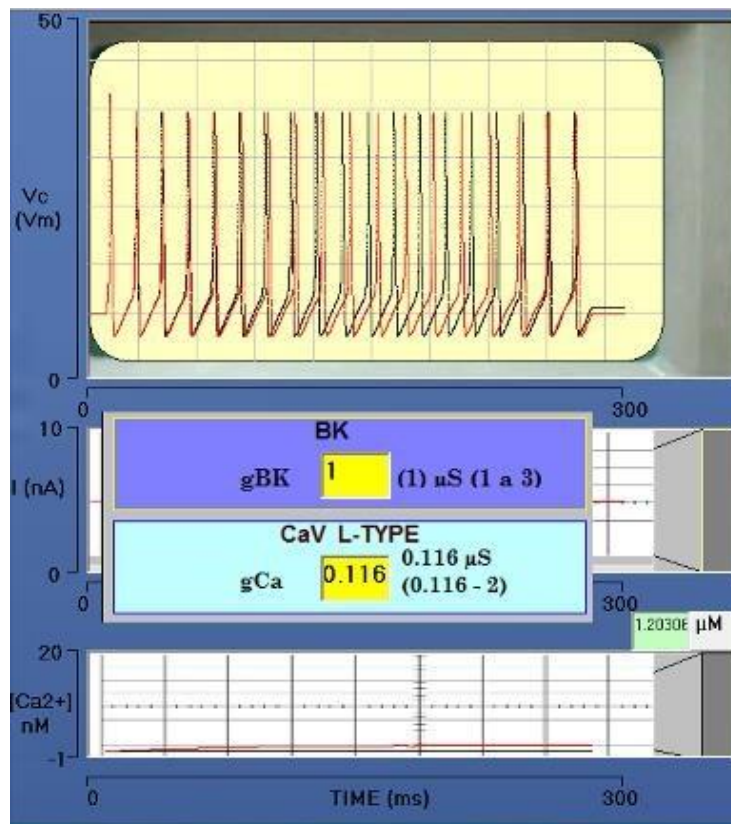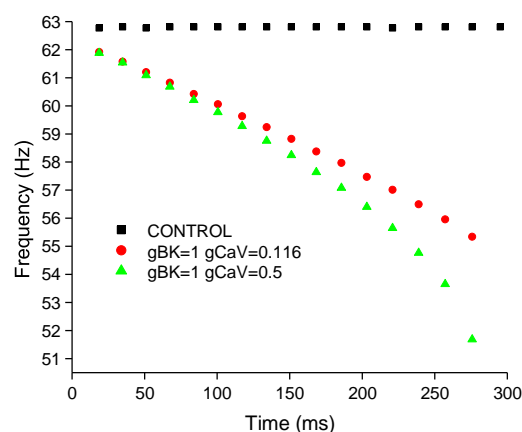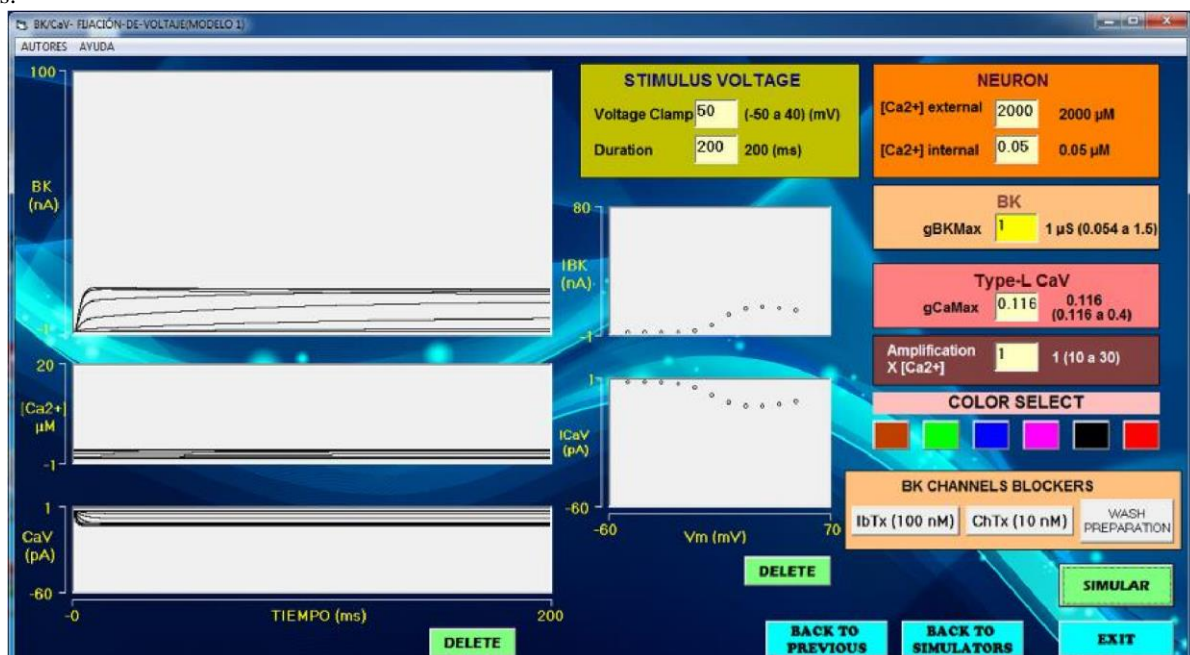

Figure 4. Frequency-time relationship. In the control neuron, it is observed how the AP frequency remains constant throughout the time of the simulation (black squares). The activation of the BK channels by the type-L CaV action ($g_{BK} = 1$ µS, $g_{Ca} = 0.116$ µS) decreases the AP frequency throughout the stimulus time (circles in red). A greater activity of the CaV channels activate more the BK channels ($g_{BK} = 1$ µS, $g_{Ca} = 0.5$ µS) producing a greater adaptation (green triangles).
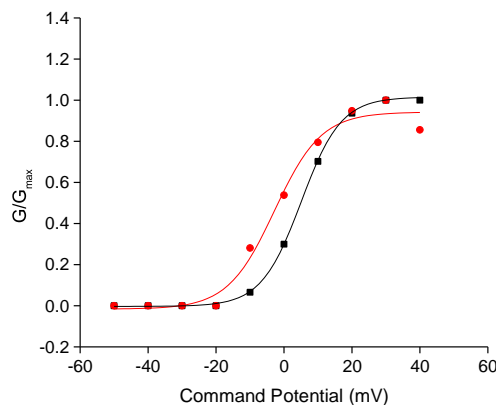
3.4 VOLTAGE CLAMP EXPERIMENTS OF THE L-TYPE CAV / BK COMPLEX

The I-V relationship for BK and CaV was explored and the Ca^{2+} concentration generated by the Ca^{2+} current was calculated (Wang, 1998). A simulator that allows carrying experiments under voltage clamp conditions was developed. The user interface has a data input module: stimulus duration and voltage, initial conditions: $[Ca^{2+}]_e$ = 2 mM, $[Ca^{2+}]_i$ = 50 nM, with g_{BK} and type-L gCaV = 1 and 0.116 µS, respectively. It has five oscilloscope screens that display: the BK current (I_{BK}), the L-type CaV current (I_{CaV}), $[Ca^{2+}]_i$, and the current-voltage relationship (I-V) for I_{BK} and I_{CaV} (Figure 5). I_{BK} and I_{CaV} currents were evoked with voltage pulses in the range of -50 to 40 mV with steps of 10 mV, V_H = -93 mV. The macroscopic I_{BK} current is displayed on the upper oscilloscope screen. An outgoing current that inactivates very slowly with time is observed (Helton et al., 2005). The macroscopic I_{CaV} current is displayed on the lower oscilloscope screen. An incoming stream that does not inactivate is observed. Changes in $[Ca^{2+}]_i$ are displayed on the intermediate oscilloscope screen. The current-voltage (I-V) curves for I_{BK} and I_{CaV} are displayed in the central part of the user interface. The I_{BK} follows the kinetics (mirrored) of I_{CaV}. The L-type CaV channel commands the BK channel (Figure 5).

Figure 5. User interface of the simulator for voltage clamp experiments. Simulation with (µS): g_{BK} = 1, g_{Ca} = 0.116. It was stimulated with voltage pulses ranging from -50 to 40 mV with steps of 10 mV. The upper oscilloscope display shows the macroscopic BK current, the middle oscilloscope display shows the internal Ca^{2+} concentration, and the lower oscilloscope shows the macroscopic Ca2+ current. The $[Ca^{2+}]_i$ increase from 0.05 to 1.87 µM. The I-V curves show how I_{BK} follows I_{CaV} kinetics.

The analysis of the conductance-voltage (G-V) normalized for BK and type-L CaV with the Boltzmann equation. Under the simulation conditions for G-V of the I_{CaV}, $V_{1/2}$ = -2.79 (mV) and for I_{BK}, $V_{1/2}$ = 5.06 (mV). First the CaV channel opens, Ca^{2+} enters the neuron, and the BK channel is activated. The G-V curve for BK follows the kinetics of the G-V curve for L-type CaV (Figure 6).

Figure 6. G-V relationship for BK and L-type CaV channels. Comparison of the G-V curves of the L-type CaV channel (red circles) and the BK channel (black squares). Experiments were performed in voltage clamp with pulses from -50 to 40 mV with steps of 10 mV. The solid lines are the fit to the Boltzmann equation at 23 ºC.

4 CONCLUSIONS

The properties of L-type Ca^{2+} channels can have important regulatory effects on the properties of action potentials. The membrane potential that regulates CaV channels may dynamically regulate the degree of activation of the BK current and produce profound effects on cell excitability. Selective coupling between L-type CaV and BK channels in the soma may provide a key mechanism that enables specific modulation of Ca^{2+} channels to exert profound physiological and pathological consequences. The decrease in cellular excitability could contain the appearance of repetitive APs that lead to disorders such as epilepsy. Under conditions where the electrophysiology of BK channels is normal, an increase in g_{Na} intensifies excitability again. The mechanisms that regulate cell excitability are complex and the precise role of ionic currents and their synchronization still requires intensive study. The BK channels are $[Ca^{2+}]_i$ sensors, a sudden increase in Ca^{2+} is the signal for their activation and to stop the AP train.

REFERENCES

Augustine, G. J., Santamaria, F., Tanaka, K., & Carolina, N. (2003). Local Calcium Signaling in Neurons Review. *Neuron*, *40*, 331–346. https://doi.org/10.1016/s0896-6273(03)00639-1

Bean, B. P. (1989). Classes of calcium channels in vertebrate cells. *Annu Rev Fisiol*, 51:367-384. https://doi.org/10.1146/annurev.ph.51.030189.002055

Bellono, N. W., Leitch, D. B., Julius, D., & Francisco, S. (2017). Molecular basis of ancestral vertebrate electroreception. *Nature*, *543*(Xxxx), 391–396. https://doi.org/10.1038/nature21401.Molecular

Bock, T., & Stuart, G. J. (2016). The impact of BK channels on cellular excitability depends on their subcellular location. *Front Cell Neurosci*, *10*(AUG), 1–8. https://doi.org/10.3389/fncel.2016.00206

Butler, A., Tsunoda, S., McCobb, D. P., Wei, A., Salkoff, L., Gautam, N., Gilman, G., & Chem, J. B. (1993). *mSlo*, a complex mouse gene encoding "Maxi" calcium-activated potassium channels. *Science*, *261*, 221–224. https://doi.org/10.1126/science.7687074

Contet, C., Goulding, S. P., Kuljis, D. A., & Barth, A. L. (2016). BK channel sin the CNS. *Int Rev Neurobiol*, 128, 281–342. https://doi.org/10.1016/bs.irn.2016.04.001.BK

Contreras, G. F., Castillo, K., Enrique, N., Carrasquel-Ursulaez, W., Castillo, J. P., Milesi, V., Neely, A., Alvarez, O., Ferreira, G., Gonzalez, C., & Latorre, R. (2013). A BK (*Slo1*) channel journey from molecule to physiology. *Channels*, *7*(6), 442–458. https://doi.org/10.4161/chan.26242

Cox, D. H. (2014). Modeling a Ca^{2+} channel/BKCa channel complex at the single-complex level. *Biophys J*, *107*(12), 2797–2814. https://doi.org/10.1016/j.bpj.2014.10.069

Cui, J., Cox, D. H., & Aldrich, R. W. (1997). Intrinsic voltage dependence and Ca^{2+} regulation of *mslo* large conductance Ca-activated K^+ channels. *J Gen Physiol*, *109*(May), 647–673. https://doi.org/10.1085/jgp.109.5.647

Cui, J., Yang, H., & Lee, U. S. (2009). Review Molecular mechanisms of BK channel activation. *CMLS*, *66*, 852– 875. https://doi.org/10.1007/s00018-008-8609-x

Galvez, A., Gimenez-Gallego, G., Reuben, J. P., Roy-Contancin, L., Feigenbaum, P., Kaczorowski, G. J., & Garcia, M. L. (1990). Purification and characterization of a unique, potent, peptidyl probe for the high conductance calcium-activated potassium channel from venom of the scorpion Buthus tamulus. *J Biol Chem*, *265*(19), 11083–11090. https://doi.org/10.13039/501100006393

Ha, G. E., & Cheong, E. (2017). Spike frequency adaptation in neurons of the central nervous system. *Exp Neurobiol*, *26*(4), 179–185. https://doi.org/10.5607/en.2017.26.4.179

Hell, J. W., Westenbroek, R. E., Warner, C., Ahlijanian, M. K., Prystay, W., Gilbert, M. M., Snutch, T. P., & Catterall, W. A. (1993). Identification and differential subcellular localization of the neuronal class C and class D L-type calcium channel α1 subunits. *J Cell Biol*, *123*(4), 949–962. https://doi.org/10.1083/jcb.123.4.949

Helton, T. D., Xu, W., & Lipscombe, D. (2005). Neuronal L-type calcium channels open quickly and are inhibited slowly. *J Neurosci*, *25*(44), 10247–10251. https://doi.org/10.1523/JNEUROSCI.1089-05.2005

Hodgkin, A. L., & Huxley, A. F. (1952). A quantitative description of membrane current and its application to conduction and excitation in Nerve. *J Physiol*, *117*(4), 500–544. https://doi.org/10.1113/jphysiol.1952.sp004764

Indriati, D. W., Kamasawa, N., Matsui, K., Meredith, A. L., Watanabe, M., & Shigemoto, R. (2013). Quantitative localization of Cav2.1 (P/Q-Type) voltage-dependent calcium channels in Purkinje cells: Somatodendritic gradient and distinct somatic Coclustering with calcium-activated potassium channels. *J Neurosci*, *33*(8), 3668–3678. https://doi.org/10.1523/JNEUROSCI.2921-12.2013

Jackson, W. F. (2018). Potassium channels in regulation of vascular smooth muscle contraction and growth. *Adv Pharmacol*, *78*, 78–89. https://doi.org/10.1016/bs.apha.2016.07.001.Potassium

Kaufmann, W. A., Ferraguti, F., Fukazawa, Y., Kasugai, Y., Shigemoto, R., Laake, P., Sexton, J. A., Ruth, P., Wietzorrek, G., Knaus, H. G., Storm, J. F., & Ottersen, O. P. (2009). Large-conductance calciumactivated potassium channels in Purkinje cell plasma membranes are clustered at sites of hypolemmal microdomains. *J Comp Neurol*, *515*(2), 215–230. https://doi.org/10.1002/cne.22066

Kshatri, A. S., Gonzalez-Hernandez, A., & Giraldez, T. (2018). Physiological Roles and Therapeutic Potential of Ca^{2+} Activated Potassium Channels in the Nervous System. *Front Mol Neurosci*, *11*(July), 1–18. https://doi.org/10.3389/fnmol.2018.00258

Lancaster, B., & Nicoll, R. A. (1987). Properties of two calcium-activated hyperpolarizations in rat hippocampal neurones. *J Physiol*, *389*(1), 187–203. https://doi.org/10.1113/jphysiol.1987.sp016653

Latorre, Ramon, Castillo, K., Carrasquel-Ursulaez, W., Sepulveda, R. V., Gonzalez-Nilo, F., Gonzalez, C., & Alvarez, O. (2017). Molecular determinants of BK channel functional diversity and functioning. *Physiol Rev*, *97*(1), 39–87. https://doi.org/10.1152/physrev.00001.2016

Lee, U. S., & Cui, J. (2010). BK channel activation : structural and functional insights. *Trends Neurosci*, *33*(9), 415–423. https://doi.org/10.1016/j.tins.2010.06.004

Li, Q., & Yan, J. (2016). Modulation of channels function by auxiliary beta and gamma subunits. *Int Rev Neurobiol*, 128, 51–90. https://doi.org/10.1016/bs.irn.2016.03.015

Marcantoni, A., Vandael, D. H. F., Mahapatra, S., Carabelli, V., Sinnegger-brauns, M. J., Striessnig, J., & Carbone, E. (2010). Loss of Cav1.3 Channels Reveals the Critical Role of L-Type and BK Channel Coupling in Pacemaking Mouse Adrenal Chromaffin Cells. *J Neurosci*, *30*(2), 491–504. https://doi.org/10.1523/JNEUROSCI.4961-09.2010

Meera, P., Wallner, M., Jiang, Z., & Toro, L. (1996). A calcium switch for the functional coupling between α (*hslo*) and β subunits (KV,Ca β) of maxi K channels. *FEBS Letters*, *382*(1–2), 84–88. https://doi.org/10.1016/0014-5793(96)00151-2

Miranda, P., Holmgren, M., & Giraldez, T. (2018). Voltage-dependent dynamics of the BK channel cytosolic gating ring are coupled to the membrane-embedded voltage sensor. *ELife*, *7*, 1–18. https://doi.org/10.7554/eLife.40664

Misonou, H., Menegola, M., Buchwalder, L., Park, E., Meredith, A., Rhodes, K., Aldrich, R., & Trimmer, J. (2006). Immunolocalization of the Ca^{2+} -activated K^+ channel Slo1 in axon and nerve terminals of mammalian brain and cultured neurons. *J Comp Neurol*, *496*(3), 289–302. https://doi.org/10.1002/cne.20931

Müller, A., Kukley, M., Uebachs, M., Beck, H., & Dietrich, D. (2007). Nanodomains of single Ca^{2+} channels contribute to action potential repolarization in cortical neurons. *J Neurosci*, *27*(3), 483–495. https://doi.org/10.1523/JNEUROSCI.3816-06.2007

Poolos, N. P., & Johnston, D. (1999). Calcium-activated potassium conductances contribute to action potential repolarization at the soma but not the dendrites of hippocampal CA1 pyramidal neurons. *J Neurosci*, *19*(13), 5205–5212. https://doi.org/10.1523/jneurosci.19-13-05205.1999

Pospischil, M., Toledo-Rodriguez, M., Monier, C., Piwkowska, Z., Bal, T., Frégnac, Y., Markram, H., & Destexhe, A. (2008). Minimal Hodgkin-Huxley type models for different classes of cortical and thalamic neurons. *Biol Cybern*, *99*(4–5), 427–441. https://doi.org/10.1007/s00422-008-0263-8

Stefani, E., Ottolia, M., Noceti, F., Olcese, R., Wallner, M., Latorre, R., & Toro, L. (1997). Voltagecontrolled gating in a large conductance Ca^{2+}-sensitive K^+ channel (*hslo*). *Proc Natl Acad Sci USA*, *94*(10), 5427–5431. https://doi.org/10.1073/pnas.94.10.5427

Sterratt, D., Graham, B., Gillies, A., & Willshaw, D. (2011). *Principles of Computational Modelling in Neuroscience*. Cambridge: Cambridge University Press.

Striessnig, J., Koschak, A., Sinnegger-Brauns, M. J., Hetzenauer, A., Nguyen, N. K., Busquet, P., Pelster, G., & Singewald, N. (2006). Role of voltage-gated L-type Ca^{2+} channel isoforms for brain function. *Biochem Soc Trans*, *34*(5), 903–909. https://doi.org/10.1042/BST0340903

Toro, L., Wallner, M., Meera, P., Tanaka, Y., & Ca, C. K. (1998). Maxi-K(Ca), a unique member of the voltage-gated K channel superfamily. *New Physiol Sci*, *13*, 112–117. https://doi.org/ 10.1152/physiologyonline.1998.13.3.112

Traub, R. D. (1982). Simulation of intrinsic bursting in CA3 hippocampal neurons. *Neuroscience*, *7*(5), 1233–1242. https://doi.org/10.1016/0306-4522(82)91130-7

Traub, R. D., Wong, R. K. S., Miles, R., & Michelson, H. (1991). A model of a CA3 hippocampal pyramidal neuron incorporating voltage-clamp data on intrinsic conductances. *J Neurophysiol*, *66*(2), 635–650. https://doi.org/10.1152/jn.1991.66.2.635

Tsien, R W, Lipscombe, D., & Madison, D. V. (1988). Multiple types of neuronal caldum channels and their selective modulation. *Trends Neurosci*, 11(10): 431-438. https://doi.org/10.1016/0166-2236(88)90194-4

Tsien, Richard W., Ellinor, P. T., & Horne, W. A. (1991). Molecular diversity of voltage-dependent Ca^{2+} channels. *Trends Pharmacol Sci*, *12*, 349–354. https://doi.org/10.1016/01656147(91)90595-J

Vivas, O., Moreno, C. M., Santana, L. F., Hille, B., & States, U. (2017). Proximal clustering between BK and CaV 1.3 channels promotes functional coupling and BK channel activation at low voltage. *eLife*, 6:e28029. https://doi.org/10.7554/eLife.28029

Wang, X. J. (1998). Calcium coding and adaptive temporal computation in cortical pyramidal neurons. *J Neurophysiol*, 79(3), 1549–1566. https://doi.org/10.1152/jn.1998.79.3.1549

Whitt, J. P., Mcnally, B. A., & Meredith, A. L. (2018). Differential contribution of Ca2+ sources to day and night BK current activation in the circadian clock. *J Gen Physiol*, 150(2), 259–275. https://doi.org/10.1085/jgp.201711945

Zill, D. G. (1988). Ecuaciones diferenciales con aplicaciones. México: *Grupo Editorial Iberoamérica*.